On the occurrence of magnetic enhancements caused by solar wind interaction with lunar crustal fields

J. S. Halekas,[1] D. A. Brain,[1] D. L. Mitchell,[1] R. P. Lin,[1] and L. Harrison[2]

Received 1 February 2006; revised 21 March 2006; accepted 30 March 2006; published 27 April 2006.

[1] We use Lunar Prospector data to identify 990 magnetic enhancements, previously termed "limb shocks" or "limb compressions", external to the lunar wake. We find that they are clearly associated with lunar crustal sources, and sometimes occur far upstream from the limb at altitudes of ~100 km. This is inconsistent with compressional disturbances convecting downstream with the solar wind, and implies that crustal fields are sometimes strong and coherent enough to produce a fluid-like interaction where compressional waves steepen to form a shock extending upstream from their source. The likelihood of observing enhancements partly depends on upstream solar wind conditions, with low proton gyroradius and low β particularly favored. Low Mach numbers, implying a larger shock standoff distance, are also favored for observations which suggest shock-like behavior. **Citation:** Halekas, J. S., D. A. Brain, D. L. Mitchell, R. P. Lin, and L. Harrison (2006), On the occurrence of magnetic enhancements caused by solar wind interaction with lunar crustal fields, *Geophys. Res. Lett.*, *33*, L08106, doi:10.1029/2006GL025931.

1. Introduction

[2] The Moon has a minimal atmosphere/exosphere and no global magnetic field, and to first order behaves as a solid obstacle to solar wind flow. The global interaction between solar wind particles and fields and the Moon has been studied in depth. As discussed by *Halekas et al.* [2005], and references therein, the lunar wake has greatly reduced plasma density, and the resulting pressure gradient across the wake boundary creates diamagnetic currents on the boundary surface, which in turn produce increased magnetic fields in the cavity and decreased fields in the surrounding expansion region where solar wind plasma begins to refill the wake. External to the wake and expansion region, various spacecraft have also observed sporadically occurring magnetic enhancements [*Ness et al.*, 1968; *Colburn et al.*, 1971; *Russell and Lichtenstein*, 1975; *Lin et al.*, 1998] which cannot be explained unless a source of back pressure is available to compress or shock the solar wind. Researchers have proposed a variety of mechanisms, but the rough association of magnetic enhancements with the known locations of crustal magnetic sources strongly suggests that crustal sources are at least partly responsible [*Sonett and Mihalov*, 1972; *Russell and Lichtenstein*, 1975]. Upstream solar wind conditions may also help determine whether an enhancement forms [*Colburn et al.*, 1971; *Whang and Ness*, 1972].

[3] Disturbances associated with crustal fields should be observed more readily near the limb, at high solar zenith angle (SZA). Though crustal fields extend above the surface, ensuring that the magnetic obstacle is not exactly parallel to the surface, at high SZA the average solar wind dynamic pressure on a crustal source should certainly be reduced, allowing disturbances to reach higher altitudes. Furthermore, as shown in Figure 1, at high SZA a compressional disturbance generated at the source and convected downstream with the solar wind can be observed at spacecraft altitude, while at lower SZA, for us to observe a disturbance, it must extend well upstream from the source, requiring compressional waves to steepen and form a coherent shock. This requires the solar wind to interact with the small crustal anomalies in a more fluid manner.

[4] Commensurate with these expectations, Explorer 35 [*Ness et al.*, 1968; *Colburn et al.*, 1971; *Sonett and Mihalov*, 1972] and the Apollo subsatellites [*Russell and Lichtenstein*, 1975] observed enhancements near the limb, potentially interpretable as compressional disturbances or shocks. Recent observations by Lunar Prospector (LP) of large magnetic enhancements at up to ~45° forward of the limb [*Lin et al.*, 1998], on the other hand, strongly suggest a shock. The physical interaction likely spans a range from minor disturbances or compressions to more shock-like behavior. For the sake of convenience, we use the term Lunar External Magnetic Enhancement (LEME) herein to describe all these features.

[5] In this work, we exploit the large volume of LP data at altitudes of 125 km or lower, along with the presence of the Wind spacecraft as an independent monitor of upstream solar wind conditions, to investigate the spatial distribution of LEMEs near the Moon, and to determine how variations in solar wind parameters affect the likelihood of observing an LEME.

2. Data and Event Selection

[6] We utilize a data set consisting of magnetic field measurements from LP and magnetic field and solar wind proton data from WIND (time-shifted to take into account the solar wind travel time between the two spacecraft, given the known spatial separation and solar wind velocity vector), from 3813 selected LP orbits for which both LP and Wind lie well outside of the terrestrial magnetosphere and magnetosheath regions, and LP and Wind magnetic field data agree well when appropriately time-shifted. This data set was previously generated for a study of the lunar wake

[1]Space Sciences Laboratory, University of California, Berkeley, California, USA.
[2]Lunar and Planetary Laboratory, University of Arizona, Tucson, Arizona, USA.

0094-8276/06/2006GL025931$05.00

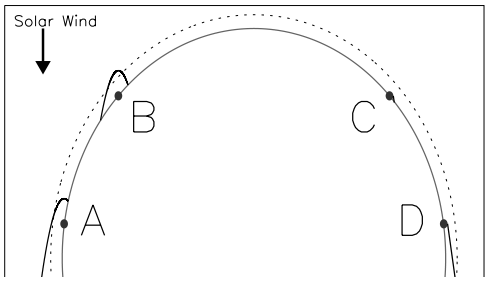

Figure 1. Cartoon showing solar wind interaction with crustal anomalies at high (A,D) and low SZA (B,C), for cases where compressional disturbances convect downstream from sources (C,D) and cases where shocks form and extend upstream from sources(A,B). Dotted line shows LP orbit.

[*Halekas et al.*, 2005], and the details of data selection are completely described therein.

[7] We search for LEMEs by comparing the LP magnetic field B with the unperturbed solar wind field B_{SW} (measured by Wind and appropriately time-shifted). We show an example LEME and the corresponding B_{SW} in Figure 2. We select only LEMEs too large to be produced by uncompressed crustal fields by using maps of crustal fields at orbital altitude [*Hood et al.*, 2001]. The LEME in Figure 2 very clearly meets this criteria, since uncompressed crustal fields at the same selenographic longitude (dashed line in Figure 2) produce only a few nT perturbation in the geomagnetic tail lobe. LEMEs must also have less than 45° of rotation from the unperturbed solar wind field direction, consistent with amplification and draping of solar wind fields, rather than direct measurements of crustal fields. Finally, we keep only LEMEs clearly separable from any surrounding magnetic noise that we often observe, especially at low altitudes, presumably due to directly measured crustal fields and/or waves (wave activity is visible throughout the LEME event in Figure 2).

[8] In the first year of the LP mission (1998), LP orbited at altitudes near 100 km, where even the largest crustal fields reach only a few nT [*Hood et al.*, 2001], and we identify 878 LEMEs on 718 out of 2501 orbits. For most of the remaining ~6 months of the mission, the LP orbital altitude lay below ~40 km, where crustal fields can reach tens of nT and we commonly observe significant magnetic noise, so we can tentatively identify only 112 LEMEs on 107 out of 1312 orbits.

3. Spatial Distribution

[9] We show all identified LEME locations, as selected above, in Figure 3, along with surface crustal fields inferred from LP Electron Reflectometer data. The 112 low-altitude LEMEs lie very near crustal sources, regardless of SZA. At high altitudes, on the other hand, 80 low-SZA LEMEs also lie very near crustal sources, but 798 high-SZA (closer to the limb) LEMEs often lie well downstream from their apparent sources. The LP polar orbit ensures that most observations near the limb also lie near the poles, explaining the polar clustering of high-SZA LEMEs, but the LP orbit does allow high-SZA observations at all latitudes twice a year. Note that all polar observations by definition lie at high SZA.

[10] Disturbances launched near the limb and convected downstream may explain high-SZA LEMEs, but cannot account for low-SZA LEMEs (see Figure 1). Some low-altitude LEMEs (especially very large ones) may represent direct measurements of compressed crustal fields, though our selection criteria should minimize these cases. However, we cannot explain high-altitude LEMEs as direct measurements of crustal fields, since we find peak LEME fields of up to tens of nT at altitudes where unperturbed crustal fields only reach a few nT (e.g., Figure 2).

[11] Unperturbed crustal fields reach a maximum of ~30 nT at ~20 km altitude [*Hood et al.*, 2001], and we require a magnetic field of ~70 nT to stop the solar wind flow, which has a typical dynamic pressure of ~2 nPa. Therefore, the altitude D_P at which magnetic pressure balances dynamic pressure should only lie at ~10 km at the subsolar point. At higher SZA, this could increase to tens of km due to the reduction in the normal component of dynamic pressure. Nearly 10% of the high-altitude observations lie at SZA < 60°, and MHD waves launched from within tens of km of any point on the lunar surface cannot reach LP. Furthermore, the close association with crustal sources demonstrates that many LEMEs are likely generated nearly directly below LP, so we actually observe them well upstream from their sources. The most likely explanation for at least the high-altitude low-SZA LEMEs is therefore a shock-like interaction.

4. Dependence on Solar Wind Parameters

[12] In Figure 4 we compare the distribution of solar wind parameters for all 3813 LP orbits with those from the 825 orbits (at all altitudes) on which we observe at least one LEME. All parameters except magnetosonic Mach number M_{MS} are calculated from Wind data as described by *Halekas et al.* [2005]. The calculation of M_{MS} requires both Alfven velocity V_A and sound speed V_S, which in turn depends on electron temperature T_e. We calculate T_e as described in *Halekas et al.* [2005] for a portion of each orbit far from crustal sources and LEMEs, and assume that it does not vary significantly on the two hour orbital time scale. We consider this a reasonable approximation since for other parameters we use orbital averages.

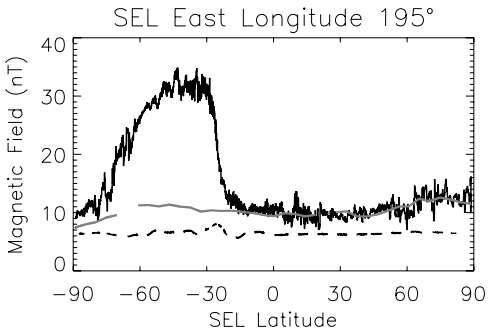

Figure 2. Large LEME observed by LP on Feb. 1, 1998 (black), corresponding B_{SW} (grey), and LP data from the geomagnetic tail lobe at the same selenographic longitude on Apr. 9, 1998 (dashed, shifted by 5 nT for clarity).

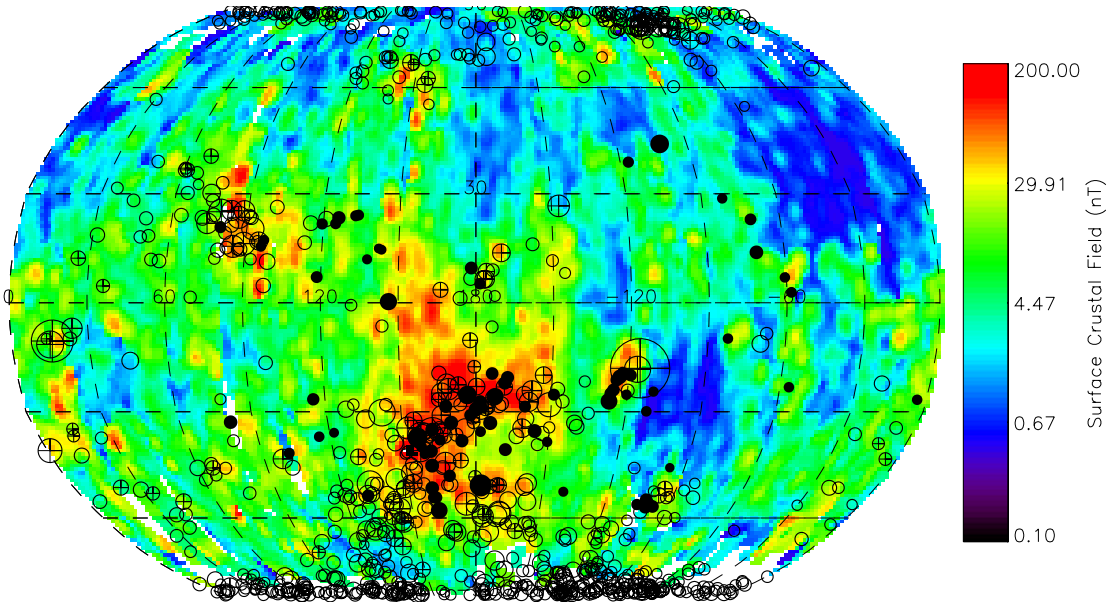

Figure 3. Circles show spacecraft location at LEME peak, with radii corresponding to compression ratio (B/B_{SW}) from 1 to 7, over a map of surface crustal fields. Crossed circles show enhancements at altitudes <75 km, open circles altitudes >75 km and SZA > 60°, and filled circles altitudes >75 km and SZA < 60°.

[13] For orbits with high-SZA LEMEs, distributions of proton density (n_P), temperature (T_P), gyroradius (R_P), and β_P differ considerably from the average solar wind distribution. Chi-square and Kolmogorov-Smirnov tests show that the chance of the latter three distributions being drawn from the same parents as the average solar wind distributions is $<10^{-20}$, while the chance for density is $<10^{-6}$. For all of these parameters, values which should make the solar wind interact with crustal sources in a more fluid manner are favored. Lower T_P and β_P ensure that the solar wind is colder and that particle effects are less important than magnetic fields. Lower R_P ensures that the crustal source scale size is larger with respect to the proton gyroradius, allowing a more fluid-like interaction. Higher n_P implies

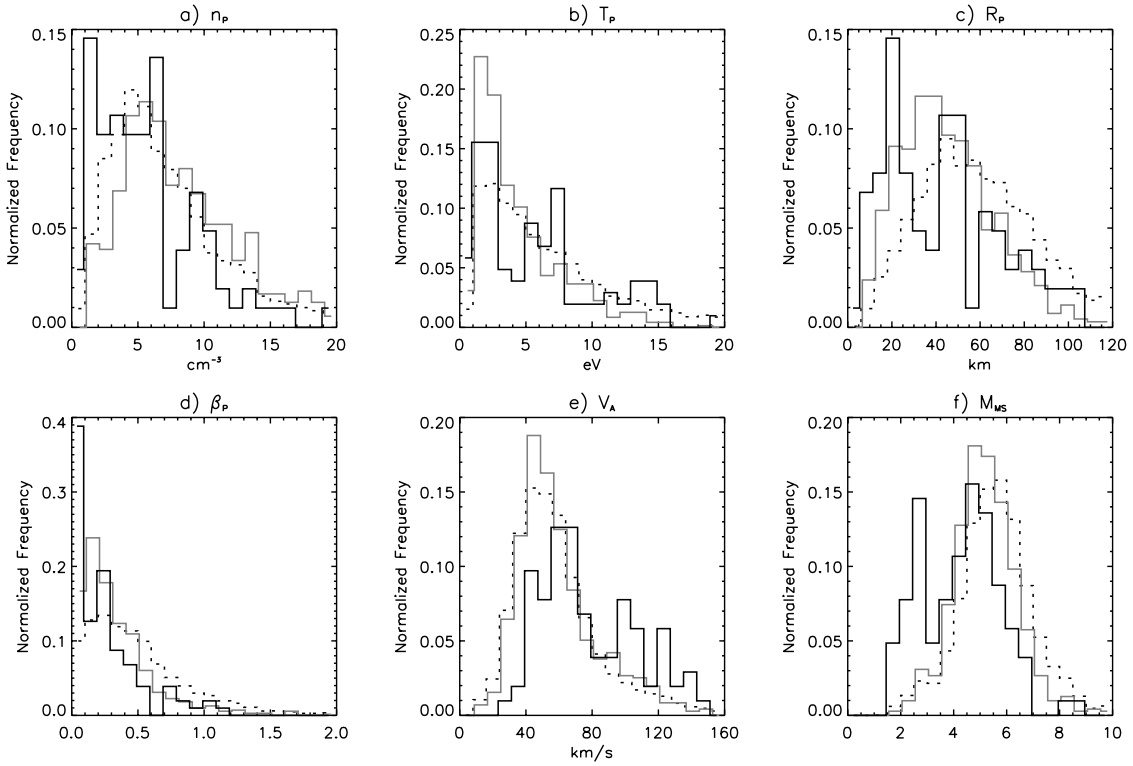

Figure 4. Dashed distributions show solar wind parameters for all LP orbits. Solid distributions correspond to orbits where we observe at least one LEME, for SZA > 60° (grey) and SZA < 60° (black).

lower proton inertial length, ensuring that D_P is larger with respect to that quantity.

[14] For orbits with low-SZA LEMEs, all distributions mentioned above except density are at least as skewed from the average solar wind distribution. The density distribution is skewed in the opposite sense, but a Chi-square test shows that there is less than a 0.1% that this distribution is the same as the average solar wind distribution, so no strong conclusions can be drawn. In addition, for low-SZA orbits, high V_A and low M_{MS} are strongly favored. In order for us to observe an LEME at LP at low SZA, it must extend above orbital altitude, unlike at high SZA where it could be generated at lower altitudes above the source but propagate at the Mach angle and be observed at higher altitudes downstream (see Figure 1). According to MHD simulations [*Cairns and Lyon*, 1996] and observations at Venus [*Tatrallyay et al.*, 1984], a lower Mach number generally implies a higher shock standoff distance, increasing the chance of observing the LEME at orbital altitude. Since low β is strongly favored, V_A should prove more important than V_S, as we observe.

[15] We have also investigated a number of other parameters, including sound speed, dynamic pressure, and the angles between the solar wind magnetic field and the solar wind velocity and surface normal. We find that none of these distributions differ as significantly from average solar wind distributions as those presented here. Other parameters, including magnetic field, solar wind velocity, and plasma pressure, do have significantly different distributions, but they vary in the manner expected from their relation to the quantities already discussed.

5. Comparison to Theory and Models

[16] *Greenstadt* [1971] discussed three necessary conditions for a magnetosphere-like interaction. The magnetic field must be strong enough to stand off the solar wind, D_P must exceed the solar wind stopping distance, and the lateral dimensions of the magnetic obstacle must be large enough that edge effects do not dominate the interaction. For lunar crustal anomalies, the first condition is easily met. Also, as discussed above, D_P is on the order of $\sim$10 km, and the stopping distance calculated in his work is a multiple of the geometric mean of proton and electron gyroradii, also on the order of tens of km, so the second condition could be met at times. Meanwhile, lateral scales must be at least a few times the proton gyroradius. The largest groups of anomalies are hundreds of km across, also satisfying this condition. It appears that all of Greenstadt's conditions can be at least marginally met at the Moon.

[17] We also compare with simulations of solar wind interaction with a dipole field [*Omidi et al.*, 2002], which show a signature that varies as dipole strength increases from no interaction, to a whistler wake, to a magnetosonic wake, to a shock-like interaction, to a magnetosphere-like interaction. They discussed their results in terms of D_P divided by the proton inertial length. For the lunar case, this number should be on the order of $\sim$0.1, which according to their results might result in a magnetosonic wake, but not a shock-like interaction. However, as other simulations show, the addition of multiple dipoles can dramatically increase the efficiency of the interaction with the solar wind [*Harnett and Winglee*, 2003]. The groups of anomalies associated with most of the LEMEs have very complicated non-dipolar morphologies [*Hood et al.*, 2001], and a lateral scale large with respect to D_P, potentially increasing the efficiency of the interaction with the solar wind.

6. Conclusions

[18] Our observations strongly suggest that at least some LEMEs are manifestations of a shock-like interaction, though many others could be explained by compressional disturbances convected downstream with the solar wind. LEMEs may span a range of behaviors encompassing both of these modes. The chance of observing an LEME varies moderately with solar wind parameters, with conditions that increase the likelihood of a fluid-like interaction with crustal magnetic sources favored. Low Mach numbers, ensuring a larger shock standoff distance, are also favored for observations that suggest shock-like behavior. The results of this study can serve as a guide for future detailed case studies of selected LEMEs, which provide us a window on the solar wind interaction with magnetic fields at scales where the interaction is on the fuzzy edge between fluid and kinetic behavior.

[19] **Acknowledgments.** This work was supported by NASA grants NNG05GH18G and NNG05GJ24G. We thank two reviewers for helpful and constructive comments.

References

Cairns, I. H., and J. G. Lyon (1996), Magnetic field orientation effects on the standoff distance of Earth's bow shock, *Geophys. Res. Lett.*, *23*, 2883–2886.

Colburn, D. S., J. D. Mihalov, and C. P. Sonett (1971), Magnetic observations of the lunar cavity, *J. Geophys. Res.*, *76*, 2940–2957.

Greenstadt, E. W. (1971), Conditions for magnetic interaction of asteroids with the solar wind, *Icarus*, *14*, 374–381.

Halekas, J. S., S. D. Bale, D. L. Mitchell, and R. P. Lin (2005), Electrons and magnetic fields in the lunar plasma wake, *J. Geophys. Res.*, *110*, A07222, doi:10.1029/2004JA010991.

Harnett, E. M., and R. M. Winglee (2003), 2.5-D fluid simulations of the solar wind interacting with multiple dipoles on the surface of the Moon, *J. Geophys. Res.*, *108*(A2), 1088, doi:10.1029/2002JA009617.

Hood, L. L., A. Zakharian, J. Halekas, D. L. Mitchell, R. P. Lin, M. H. Acuña, and A. B. Binder (2001), Initial mapping and interpretation of lunar crustal magnetic anomalies using Lunar Prospector data, *J. Geophys. Res.*, *106*, 27,825–27,840.

Lin, R. P., D. L. Mitchell, D. W. Curtis, K. A. Anderson, C. W. Carlson, J. McFadden, M. H. Acuña, L. L. Hood, and A. Binder (1998), Lunar surface magnetic fields and their interaction with the solar wind: Results from Lunar Prospector, *Science*, *281*, 1480–1484.

Ness, N. F., K. W. Behannon, H. E. Taylor, and Y. C. Whang (1968), Perturbations of the interplanetary magnetic field by the lunar wake, *J. Geophys. Res.*, *73*, 3421–3440.

Omidi, N., X. Blanco-Cano, C. T. Russell, H. Karimabadi, and M. Acuña (2002), Hybrid simulations of solar wind interaction with magnetized asteroids: General characteristics, *J. Geophys. Res.*, *107*(A12), 1487, doi:10.1029/2002JA009441.

Russell, C. T., and B. R. Lichtenstein (1975), On the source of lunar limb compression, *J. Geophys. Res.*, *80*, 4700–4711.

Sonett, C. P., and J. D. Mihalov (1972), Lunar fossil magnetism and perturbations of the solar wind, *J. Geophys. Res.*, *77*, 588–603.

Tatrallyay, M., C. T. Russell, J. G. Luhmann, A. Barnes, and J. D. Mihalov (1984), On the proper Mach number and ratio of specific heats for modeling the Venus bow shock, *J. Geophys. Res.*, *89*, 7381–7392.

Whang, Y. C., and N. F. Ness (1972), Magnetic-field anomalies in the lunar wake, *J. Geophys. Res.*, *77*, 1109–1115.

D. A. Brain, J. S. Halekas, R. P. Lin, and D. L. Mitchell, Space Sciences Laboratory, University of California, Berkeley, CA 94720, USA. (jazzman@ssl.berkeley.edu)

L. Harrison, Lunar and Planetary Laboratory, University of Arizona, Tucson, AZ 85721, USA.